Proc. Natl. Acad. Sci. USA
Vol. 92, pp. 3754–3758, April 1995
Genetics

The W^{sh} and *Ph* mutations affect the c-*kit* expression profile: c-*kit* misexpression in embryogenesis impairs melanogenesis in W^{sh} and *Ph* mutant mice

REGINA DUTTLINGER*†, KATIA MANOVA*‡, GEORGINA BERROZPE*, TANG-YANG CHU*§, VICTOR DELEON‡, INNA TIMOKHINA*, RAJU S. K. CHAGANTI¶, ANDREW D. ZELENETZ*, ROSEMARY F. BACHVAROVA‡, AND PETER BESMER*‖

*Molecular Biology and ¶Cell Biology and Genetics Programs, Memorial Sloan–Kettering Institute and Cornell University Graduate School of Medical Sciences, New York, NY 10021; and ‡Department of Cell Biology and Anatomy, Cornell University Medical College, New York, NY 10021

Communicated by David E. Housman, Massachusetts Institute of Technology Center for Cancer Research, Cambridge, MA, January 3, 1995

ABSTRACT **The receptor tyrosine kinases (RTKs) c-*kit* and platelet-derived growth factor receptor α chain (PDGFRa) are encoded at the white spotting (*W*) and patch (*Ph*) loci on mouse chromosome 5. While *W* mutations affect melanogenesis, gametogenesis, and hematopoiesis, the *Ph* mutation affects melanogenesis and causes early lethality in homozygotes. *W*-sash (W^{sh}) is an expression mutation and blocks c-*kit* expression in certain cell types and enhances c-*kit* expression in others, including at sites important for early melanogenesis. We have determined the effect of *Ph* on c-*kit* expression during embryogenesis in *Ph* heterozygotes. Immunohistochemical analysis revealed enhanced c-*kit* expression in several cell types, including sites important for early melanogenesis. We propose that in both W^{sh} and *Ph* mutant mice c-*kit* misexpression affects early melanogenesis and is responsible for the pigment deficiency. Moreover, we have defined the organization of the RTKs in the *W/Ph* region on chromosome 5 and characterized the W^{sh} mutation by using pulsed-field gel electrophoresis. Whereas the order of the RTK genes was determined as *Pdgfra*–c-*kit*–*flk1*, analysis of the W^{sh} mutation revealed that the c-*kit* and *Pdgfra* genes are unlinked in W^{sh}, presumably because of an inversion of a small segment of chromosome 5. The *Ph* mutation consists of a deletion including *Pdgfra* and the 3′ deletion endpoint of *Ph* lies between *Pdgfra* and c-*kit*. Therefore, positive 5′ upstream elements controlling c-*kit* expression in mast cells and some other cell types are affected by the W^{sh} mutation and negative elements are affected by both the W^{sh} and the *Ph* mutation.**

The closely linked white spotting (*W*), patch (*Ph*), and *Rw* mutations all have distinctive pigmentation phenotypes (1). *W* mutations have been studied extensively because of their pleiotropic effects on melanogenesis, gametogenesis, and hematopoiesis (for reviews, see refs. 2 and 3). The *Ph* mutation has severe effects on mesenchymal tissues in early embryonic development and causes lethality in homozygotes; in addition, the *Ph* mutation affects melanogenesis (4–7). The murine *W* locus encodes the c-*kit* receptor tyrosine kinase (RTK) (8–10), whereas *Ph* encodes the platelet-derived growth factor (PDGF) receptor α chain (PDGFRa) (11, 12). Moreover, another RTK, *flk1*, maps in the vicinity of the *W/Ph/Rw* complex on mouse chromosome 5 (13).

Many different *W* mutations have been identified and characterized. These mutations vary in their degree of severity in the heterozygous and the homozygous state, but most affect the different cellular targets similarly (2, 14, 15). The molecular characterization of these *W* mutations indicates that they are null mutations or that they impair the intrinsic Kit receptor function to differing degrees (10, 16–18). *W*-sash (W^{sh}) is another type of mutation. It affects only pigmentation and tissue mast cells and therefore W^{sh} mutant mice are fertile and not anemic, but they are black-eyed whites and lack tissue mast cells (19, 20). Heterozygotes have a broad white sash/belt in the trunk region. W^{sh} is a mutation that affects c-*kit* expression in a tissue-specific manner during embryonic development and in the adult (21, 22). While the mast cell deficiency in W^{sh} mice results from lack of c-*kit* expression, enhanced c-*kit* expression in somitic dermatomes at the time of melanoblast migration from the neural crest to the periphery may cause the pigmentation defect. The abnormal c-*kit* expression in W^{sh} mutant mice has been suggested to affect early melanogenesis in a dominant fashion. Analysis of chromosomal DNA from W^{sh}/W^{sh} mice indicated a deletion or rearrangement in the vicinity of the c-*kit* gene in agreement with the fact that several control elements are affected by this mutation (21).

Mice heterozygous for the *Ph* mutation display a pigmentation pattern very similar to $W^{sh}/+$ mice, while homozygous *Ph/Ph* mice die during embryonic development. The *Ph* mutation arose as a result of a deletion that includes *Pdgfra* (11, 12). The 3′-deletion endpoint in the *Ph* allele, which is in juxtaposition with the c-*kit* gene, is not known precisely, but it does not include c-*kit* coding sequences. Because of the similar heterozygous pigmentation phenotypes of the W^{sh} and *Ph* mutations, we hypothesized that the pigmentation defect in *Ph*/+ mice is the result of inappropriate c-*kit* expression similar to that in $W^{sh}/+$ mice and that both mutations affect some of the same 5′ control elements of the c-*kit* gene (21, 23).

In this report, we have examined the effect of the *Ph* mutation on c-*kit* expression during embryogenesis in *Ph* heterozygotes. We show that c-*kit* expression is enhanced in several cell types, including sites important for early melanogenesis in agreement with the notion that inappropriate c-*kit* expression in *Ph* mutant mice affects early melanogenesis. We have also characterized the organization of the RTKs in the *W/Ph* region on chromosome 5 and characterized the W^{sh} mutation by analyzing megabase DNA using pulsed-field gel electrophoresis (PFGE). Our results imply that positive upstream elements controlling c-*kit* expression in mast cells and some other cell types are affected by the W^{sh} mutation and that negative upstream elements are affected by both the W^{sh} and the *Ph* mutations.

MATERIALS AND METHODS

Mice. C57BL/6J and C57BL/6*Ph*/+ mice were purchased from The Jackson Laboratory. C57BL/6 W^{sh}/W^{sh} were kindly

The publication costs of this article were defrayed in part by page charge payment. This article must therefore be hereby marked "*advertisement*" in accordance with 18 U.S.C. §1734 solely to indicate this fact.

Abbreviations: PFGE, pulsed-field gel electrophoresis; E, embryonic day.

†Present address: Roche Institute for Molecular Biology, Nutley, NJ 07110.
§Present address: Department of Obstetrics and Gynecology, Tri-Service General Hospital, Taipei, Taiwan.
‖To whom reprint requests should be addressed.

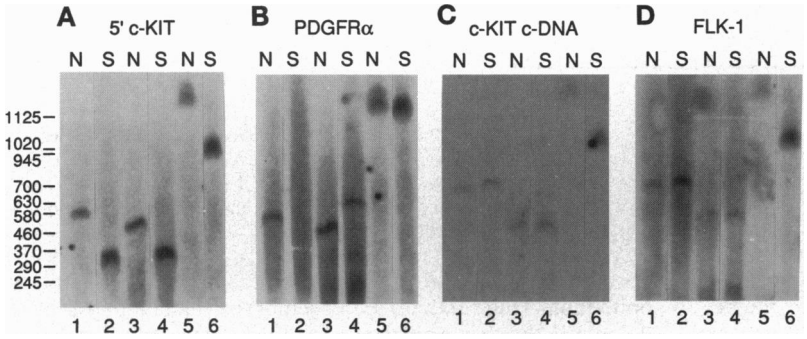

FIG. 1. Analysis of W^{sh}/W^{sh} and +/+ DNA resolved by PFGE. DNA from spleen cells of normal (lanes N) and W^{sh}/W^{sh} (lanes S) mice in agarose plugs was digested with the enzymes *Not* I (lanes 1 and 2), *Nar* I (lanes 3 and 4), and *Nru* I (lanes 5 and 6). The blot was hybridized sequentially to the 5′ c-*kit* probe (*A*), the *Pdgfra* probe (*B*), the c-*kit* cDNA probe (*C*), and the *flk1* cDNA probe (*D*). Migration of *Saccharomyces cerevisiae* chromosomes as size markers is indicated (kb).

provided by Rudolf Jaenisch (Massachusetts Institute of Technology, Cambridge).

PFGE. The preparation of samples for PFGE, enzyme digestions, and electrophoresis were prepared as described (21, 24). DNA fractionated by PFGE was transferred to nylon membranes (Zetabind; AMF Cuno) and crosslinked to filters with UV in a Stratalinker (Stratagene), and hybridization was performed as described (21). The following probes were used: a murine c-*kit* upstream probe (−617 to +37) (5′ c-*kit*) (25), a 3.7-kb murine c-*kit* cDNA probe, which includes the entire coding sequence, a 2.8-kb murine *flk1* cDNA probe (kindly provided by I. Lemischka, Princeton University), and a 600-bp *Pdgfra* cDNA probe including sequences downstream of the second tyrosine kinase domain and 3′ untranslated sequences prepared by PCR with the primers 5′-CCACCTCAGCGAGA TACTGG-3′ and 5′-TCGCGGGAACTTTCTCTCTC-3′. Probes for hybridization were labeled with [^{32}P]dCTP by the random primer method.

Immunohistochemistry. Antibodies and immunohistochemistry procedures were essentially as described (21, 26, 27). Dissected embryos were washed twice in 0.1 M sodium phosphate buffer (pH 7) and embedded in OCT (Tissue Tek, Miles). Cryostat sections were cut at 10 μm and stained with the Vectastain Elite ABC kit (Vector Laboratories). The manufacturer's instructions for the procedure were followed except that quenching of endogenous peroxidase was carried out in 0.1% H_2O_2 in phosphate-buffered saline (PBS) for 15 min, and incubation in 10% normal goat serum in PBS with 2% bovine serum albumin for 30 min was included as a blocking step for the secondary antibody, as well as an extra step to block nonspecific binding using the avidin/biotin blocking kit from Vector Laboratories. Some sections were counterstained with Harris' hematoxylin, dehydrated, and mounted in permount.

RESULTS

Long-Range Restriction Map of the *Pdgfra*, c-*kit*, and *flk1* Locus and Structural Basis of the W^{sh} Mutation. To determine the structure of the c-*kit*, *Pdgfra*, and *flk1* loci and to characterize the basis of the W^{sh} mutation, blots obtained after resolution of megabase DNA by PFGE and digested with the restriction enzymes *Not* I, *Nar* I, and *Nru* I were hybridized sequentially with a *Pdgfra* probe, an upstream c-*kit* probe (5′ c-*kit*), a c-*kit* cDNA probe, and a *flk1* cDNA probe. Hybridization of blots containing +/+ DNA with both the 5′ c-*kit* and *Pdgfra* probes resulted in *Not* I, *Nar* I, and *Nru* I fragments of 580, 500, and 1200 kb, respectively (Fig. 1). The c-*kit* and *flk1* cDNA probes both detected the 1200-kb *Nru* I fragment, which was also detected by the 5′ c-*kit* and the *Pdgfra* probes and a 630-kb *Not* I fragment. In addition, the c-*kit* probe detected *Nar* I fragments of 500 (light, partial digest) and 460 kb, whereas the *flk1* probe detected only the 500-kb fragment. In addition, *Nar* I and *Not* I sites had been placed in exon one and intron one of the *Kit* gene, respectively (25). Taken together, these results establish the order of the three receptor tyrosine kinase genes on mouse chromosome 5 as *Pdgfra*–c-*kit*–*flk1*. To generate a more detailed restriction map of the segment between c-*kit* and *Pdgfra*, double digests with *Not* I/*Mlu* I, *Not* I/*Sal* I, and *Not* I/*Nru* I were analyzed (Fig. 2). Hybridization of the *Not* I/*Sal* I double digest with the 5′ c-*kit* probe produced a 180-kb fragment, whereas the *Pdgfra* probe detected a fragment of 330 kb. Thus, a *Sal* I site lies between c-*kit* and *Pdgfra*. In addition, these experiments indicated that the *Not* I fragment includes restriction sites for *Nar* I, *Nru* I, *Mlu* I, and *Spo* I (Fig. 3).

The W^{sh} mutation stems from an inversion or deletion of sequences in the vicinity of the c-*kit* locus (21). To further define the structural basis of the W^{sh} mutation, we analyzed W^{sh}/W^{sh} DNA digested with various restriction enzymes by PFGE and sequential hybridization of blots with the *Pdgfra*, 5′ c-*kit*, c-*kit* cDNA, and *flk1* cDNA probes (Fig. 1). While the 5′ c-*kit* probe revealed W^{sh}/W^{sh} DNA fragments with *Not* I, *Nar* I, and *Nru* I smaller than those from normal DNA, the c-*kit* cDNA and the *flk1* probes detected *Not* I and *Nar* I fragments indistinguishable from normal DNA, indicating that the W^{sh} mutation affects sequences upstream of c-*kit*. Since the *Nru* I fragment includes *Pdgfra*, c-*kit*, and *flk1*, the c-*kit* cDNA and *flk1* cDNA probes detected a smaller *Nru* I fragment in W^{sh}/W^{sh} DNA. In contrast, the *Pdgfra* probe detected distinct *Nar* I and *Nru* I fragments of 700 and 1150 kb, respectively; a *Not* I fragment was not resolved under the conditions used. Furthermore, analysis of *Not* I/*Sal* I double digests with the 5′ c-*kit* probe detected a 100-kb W^{sh}/W^{sh} DNA fragment compared to a 180-kb fragment in +/+ DNA (Fig. 2*A*). By contrast, the *Pdgfra* probe detected the same 330-kb fragment in +/+ and in W^{sh}/W^{sh} DNA (Fig. 2*B*). These results suggested that the W^{sh} mutation unlinks *Pdgfra* from c-*kit* and that the breakpoint lies downstream of the *Sal* I site, presumably not more than 100 kb from c-*kit* (Fig. 3).

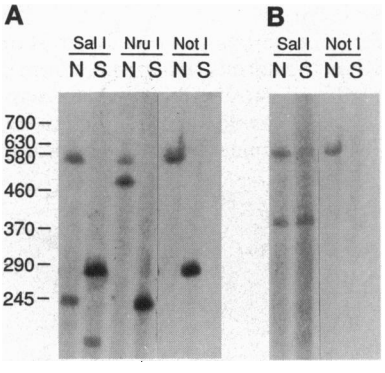

FIG. 2. *Not* I double digests of +/+ (lanes N) and W^{sh}/W^{sh} (lanes S) DNA. DNA from W^{sh}/W^{sh} and +/+ mice was digested with *Not* I/*Sal* I, *Not* I/*Nru* I, and with *Not* I alone and fractionated by PFGE with a pulse time of 1.79–54.17 s for 27 hr. The blot was hybridized sequentially with the 5′ c-*kit* (*A*) and *Pdgfra* (*B*) probes. The *Not* I/*Sal* I and *Not* I/*Nru* I double digests show in addition to a new band also the *Not* I fragment, indicating that *Nru* I and *Sal* I digestion is incomplete. Migration of size markers is indicated (kb).

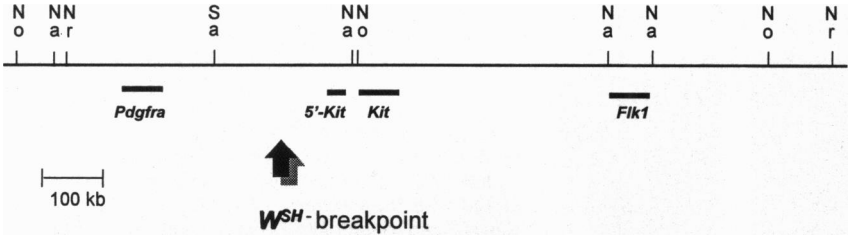

FIG. 3. Restriction map of *W*/c-*kit* locus. Sites for the restriction enzymes *Not* I (No), *Nar* I (Na), and *Nru* I (Nr) and a *Sal* I (Sa) site in between *Pdgfra* and c-*kit* and the relative W^{sh} breakpoint are indicated.

c-*kit*-Encoded Protein Misexpression in *Ph*/+ Embryos. To test whether the pigmentation defect in *Ph*/+ mice might result from inappropriate c-*kit* expression as in W^{sh}/+ mice, rather than from a half dose of PDGFRa, we determined c-*kit*-encoded protein expression patterns in embryonic day (E) 10.5, E11.5, and E13.5 *Ph*/+ embryos. *Ph*/+ embryos were obtained by mating *Ph*/+ × *Ph*/+ mice. DNA was extracted from the head or yolk sac of embryos for genotyping by slot blot analysis and sequential hybridization with *Pdgfra* and c-*kit* probes to identify *Ph*/+ embryos hemizygous for *Pdgfra* DNA content (Fig. 4), while the remaining part of the embryos was embedded for expression studies. Immunohistochemical analysis of *Ph*/+ embryos using anti-kit antibody revealed abnormal c-*kit* expression at some of the same sites as in W^{sh} mutant mice and in some other sites.

At E10.5 the most striking feature of *Ph*/+ embryos was strong expression of c-*kit*-encoded protein in the dorsal half of the neural tube (Fig. 5*B*), while in wild-type embryos a low level of uniformly distributed c-*kit*-encoded protein was present within the neural tube (Fig. 5*A*). The abnormal dorsal c-*kit* expression was present throughout the length of the neural tube except that in anterior trunk regions the roof plate was devoid of c-*kit*-encoded protein. A similar pattern of c-*kit* expression was also present in the wavy neural tube of *Ph*/*Ph* embryos (Fig. 5*C*). In the dermatome of *Ph*/+ embryos, c-*kit* was overexpressed relative to the very low level in wild-type embryos (compare Fig. 5 *D* and *E*) and expression was also abnormally high in the mesentery of the foregut (data not shown). Both wild-type and mutant embryos show strong expression in the mesenchyme around the dorsal aorta, in the hindgut mesentery, and in primordial germ cells and melanoblasts. In E11.5 *Ph*/+ embryos c-*kit* expression was similar to that at E10.5, including enhanced expression in the neural tube, dermatome, and developing dermis and the mesenchyme around the stomach (Fig. 6). Interestingly, there was no ectopic expression in recently formed dermatomes located in the tail region. Importantly, in E11.5 *Ph*/+ embryos, melanoblasts present in the skin ectoderm were reduced in number to ≈50% compared to wild type.

At E13.5 *Ph*/+ embryos continued to show enhanced expression of Kit in the dermis, which arises from dermatomes, in the trunk, head, and, most strikingly, in the ear (Fig. 7 *A*, *B*, *E*, and *F*). Also there was distinct accumulation of Kit in the dermis around the mammary gland, while both mutant and normal embryos had a low level of Kit in the mammary epithelium (Fig. 7*D*). In E13.5 embryos, melanoblasts have colonized the skin epidermis and many have well developed cell processes. In comparison to wild type, there is a significant reduction in the density of epidermal melanoblasts in *Ph*/+ embryos in the head and trunk. In the ear it was difficult to assess the number of melanoblasts in mutant animals because of the strong expression in the dermis. And there is a reduction of Kit-expressing cells in the dermis, which presumably include both melanoblast and mast cell progenitors.

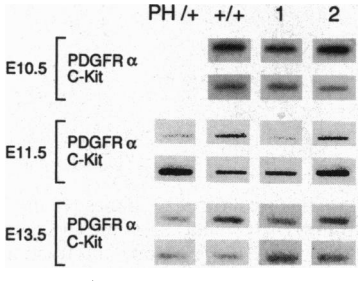

FIG. 4. Determination of genotype of embryos from *Ph*/+ × *Ph*/+ matings by slot blot analysis. DNA from *Ph*/+ and +/+ mice and from embryos were processed for slot blotting, and blots were sequentially hybridized with *Pdgfra* and c-*kit* probes.

DISCUSSION

Pdgfra, c-*kit*, and *flk1* had been shown to be closely linked. Our megabase analysis confirms and defines more precisely the organization of the *Pdgfra*–c-*kit*–*flk1* region. *Pdgfra* is ≈180–500 kb 5′ of c-*kit*, and *flk1* is 400 kb 3′ of c-*kit*; these results are in agreement with a recently published study (28). Whether there are other genes between c-*kit* and *Pdgfra* and/or c-*kit* and *flk1* is not known.

The characterization of the W^{sh} mutation is particularly interesting because this mutation affects the tissue-specific expression of the c-*kit* protooncogene and, consequently, serves as a tool in defining control elements of the c-*kit* promotor. Previous analysis indicated no deletions or other gross rearrangements of c-*kit* exon and intron sequences in W^{sh}/W^{sh} DNA and that the c-kit^{Wsh} coding sequences are unaltered (21, 22). Our PFGE analysis showed that in W^{sh}/W^{sh} DNA, sequences upstream of c-*kit* are altered and that the c-*kit* and *Pdgfra* genes are unlinked. These results can be explained by a translocation or an inversion. We hypothesize that the W^{sh} mutation is an inversion rather than a translocation and, furthermore, that in W^{sh} the c-*kit* gene is inverted. The original animals carrying the W^{sh} mutation also carried a recessive lethal mutation (*l*), which maps 1.7 centimorgans distal to *W* (19). The viable W^{sh} allele may have arisen as a consequence of a recombination event, possibly involving gene conversion or a double crossover, at the inversion breakpoint near the lethal locus. This would suggest that the second breakpoint is near the lethal locus, thus defining the size of the inverted segment. Since the second breakpoint is distal to *W*, c-*kit* and not *Pdgfra* should be inverted. In agreement with these predictions, analysis of metaphase chromosomes did not resolve the alteration (data not shown). The breakpoint between c-*kit* and *Pdgfra* is distal of the *Sal* I site between c-*kit* and *Pdgfra*. Additional experiments are necessary to clarify the exact molecular nature of the W^{sh} mutation.

Enhanced expression of c-*kit* in dermatomes of E10.5 and E11.5 W^{sh}/W^{sh} and W^{sh}/+ embryos and in the dermis at later stages is thought to provide an explanation for the dominant pigmentation defect in heterozygous and homozygous adult mutant mice (21, 23). We have analyzed c-*kit* expression patterns in *Ph*/+ embryos to determine whether a similar mechanism is responsible for the pigmentation deficiency in *Ph*/+ mice. In E10.5 embryos, c-*kit* expression was shown to be enhanced in the neural tube, somitic dermatomes, and mesentery of the foregut; at E11.5 c-*kit* expression was seen in dermatomes, the forming dermis, and the mesenchyme around the stomach; at E13.5 c-*kit* expression was observed in the

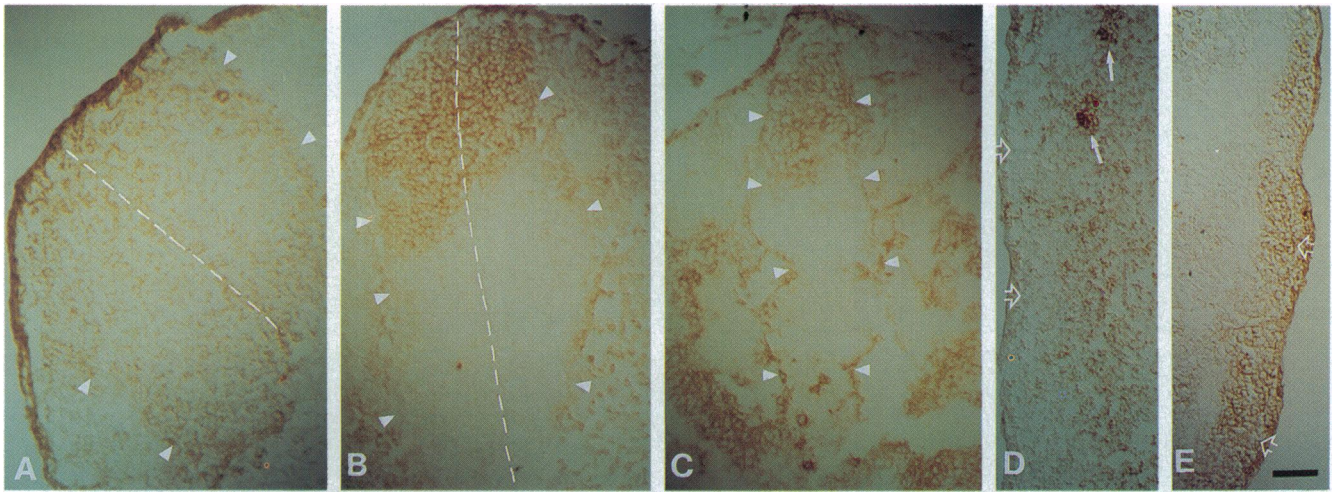

FIG. 5. Immunohistochemical analysis of c-*kit* expression at E10.5. (*A–C*) Sections through the spinal cord of wild-type, *Ph*/+, and *Ph*/*Ph* embryos, respectively. Dashed lines indicate midline of the spinal cord (indistinguishable in the *Ph*/*Ph* embryo). Arrowheads point to lateral borders of the spinal cord. (*D* and *E*) Longitudinal sections through the trunk of wild-type and *Ph*/+ embryos, respectively. Open arrows show somitic dermatomes; solid arrows in *D* indicate Kit-expressing migratory neural crest cells, possibly melanoblasts. (Bar = 50 μm.)

developing dermis of the skin in both trunk and head. Differences in c-*kit* expression in *Ph*/+ and normal embryos were particularly distinct in the dermis around the mammary gland. Although the pattern of c-*kit* misexpression in *Ph*/+ embryos differs from that in W^{sh}/W^{sh} and $W^{sh}/+$ embryos, misexpression in the dermatomes and dermis is similar and it may affect early melanogenesis in these animals by a mechanism similar to that in W^{sh}/W^{sh} and $W^{sh}/+$ animals. In agreement with this notion in *Ph*/+ embryos melanoblasts in the dermis at E11.5 and E13.5 were reduced in number in both head and trunk of *Ph*/+ embryos.

Although the finding of enhanced c-*kit* expression in *Ph*/+ embryos may explain the pigmentation defect in these mice, it cannot be ruled out that 50% dosage of *Pdgfra* receptors may affect melanogenesis and contribute to the pigmentation defect. *Pdgfra* is expressed in the dorsal region of the closing neural tube (5, 7) and derivatives of the cranial neural crest are missing in *Ph*/*Ph* embryos, indicating a direct role for *Pdgfra* in neural crest cell development (6). In E9.5 *Ph*/*Ph* embryos, mesenchymal cells in the interstitial spaces through which melanocyte precursors migrate are virtually absent and the skin of E14.5 *Ph*/*Ph* embryos is devoid of a dermal layer. Therefore, *Pdgfra* may influence melanogenesis indirectly by affecting the microenvironment of melanoblasts in the migratory pathway as well as at the final destination. However, conversely there is no evidence that the W^{sh} phenotype could be explained in part by an effect on Pdgfra; E13.5 W^{sh}/W^{sh} mutant embryos display the normal Pdgfra expression pattern as determined by immunohistochemistry (unpublished data).

The pattern of c-*kit* expression in W^{sh} and *Ph* mutant mice allows for a number of conclusions regarding the transcriptional control of c-*kit*. As a result of the proposed inversion in the W^{sh} allele, c-*kit* expression is shut off in some cell types but not in others (21). Thus, positive upstream regulatory elements controlling c-*kit* expression in mast cells and mesenchymal cells in the lung and digestive tract located at or beyond the breakpoint of the inversion are affected by the W^{sh} mutation. In addition, negative upstream c-*kit* control elements are affected by both the W^{sh} and the *Ph* mutation, while others are affected uniquely by the W^{sh} mutation or by the *Ph* mutation. While misexpression in dermatomes and in the mesenchyme of the gastrointestinal tract is seen in both W^{sh} and *Ph* embryos,

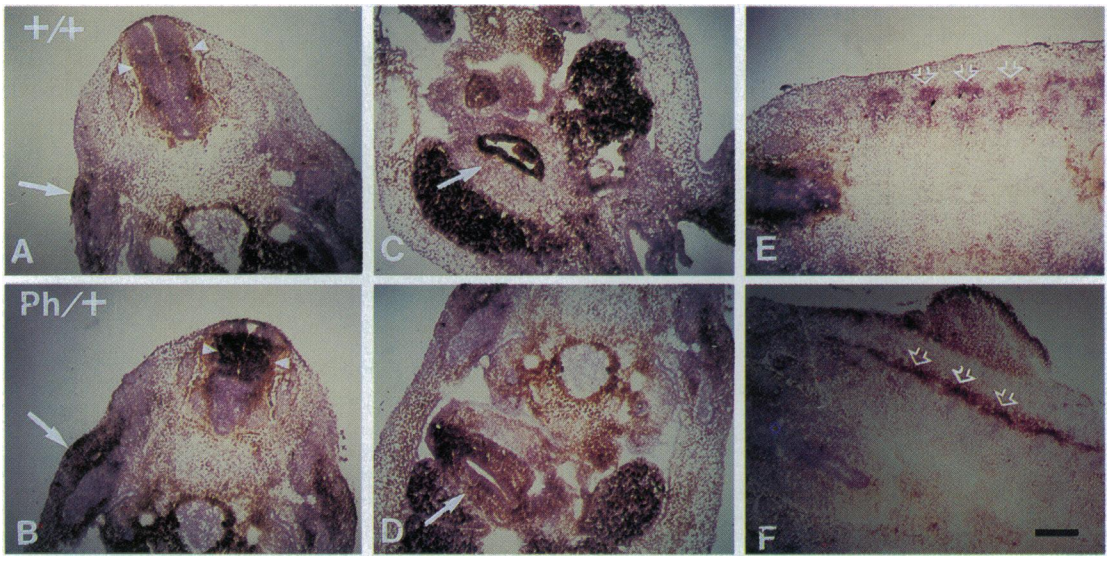

FIG. 6. Immunohistochemical analysis of c-*kit* expression at E11.5. (*A*, *C*, and *E*) Sections at different levels of the trunk of wild-type embryos. (*B*, *D*, and *F*) Sections at similar levels of *Ph*/+ embryos. (*A* and *B*) Arrowheads show lateral walls of the spinal cord; arrows point to Kit-expressing dermis of the hindlimb. (*C* and *D*) Arrows point to wall of the stomach. (*E* and *F*) Open arrows indicate a row of somitic dermatomes. (Bar = 200 μm.)

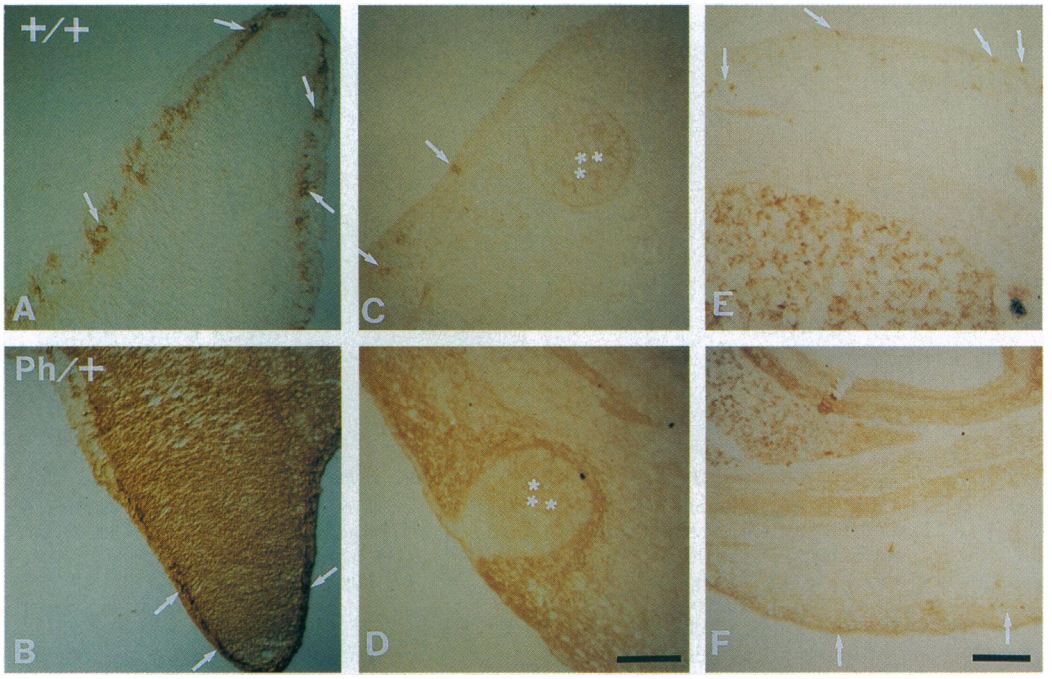

FIG. 7. Immunohistochemical analysis of c-*kit* expression. (*A*, *C*, and *E*) Sections of wild-type embryos. (*B*, *D*, and *F*) Sections taken at similar levels from *Ph*/+ embryos. (*A* and *B*) Ear pinna. Arrows point to epidermal melanoblasts. (*C* and *D*) Mammary glands. Asterisks indicate mammary epithelium; arrows point to presumptive melanoblasts and/or mast cells. (*E* and *F*) Cross sections in the region of the liver. Arrows mark melanoblasts in the epidermis and presumptive melanoblasts and/or mast cells in the dermis. (Bar in *D* = 50 μm for *A–D*; bar in *F* = 200 μm for *E* and *F*.)

expression in the floorplate and the dorsal neural tube is unique for W^{sh} and *Ph*, respectively. Expression of c-*kit* in these diverse sites may normally be turned off by an upstream silencer and this silencer is deleted or displaced in the W^{sh} and *Ph* genomes.

Rump white (*Rw*) is a radiation-induced dominant spotting mutation that is closely linked to the *W* locus (1). Heterozygous *Rw*/+ animals display depigmentation of the posterior trunk and when homozygous the mutation is lethal during midgestation. *Rw* was recently shown to be associated with an inversion involving one-third of mouse chromosome 5 and a distal breakpoint of the inversion was mapped to a region between c-*kit* and *Pdgfra* (28). It is then probable that the inversion in the *Rw* allele affects upstream c-*kit* control elements similar to the W^{sh} inversion and the *Ph* deletion, and c-*kit* misexpression at sites important for early melanogenesis is a likely consequence. The characterization of the breakpoints of the W^{sh}, *Ph*, and *Rw* mutations should provide important insight into the mechanisms governing c-*kit* expression.

We would like to thank Drs. William Hayward, Tony Brown, and Elizabeth Lacy for numerous discussions, Ihor Lemischka for the *flk1* probe, and Daniel Bowen-Pope for Pdgfra antibody. Support by grants from the National Cancer Institute, National Institute of Child Health Development, and from the National Science Foundation is acknowledged.

1. Searle, A. G. & Truslove, G. M. (1970) *Genet. Res.* **15**, 227–235.
2. Silvers, W. K. (1979) *The Coat Colors of Mice* (Springer, New York).
3. Russell, E. S. (1979) *Adv. Genet.* **20**, 357–459.
4. Grueneberg, H. & Truslove, G. M. (1960) *Genet. Res.* **1**, 69–90.
5. Orr-Urtreger, A., Bedford, M. T., Do, M. S., Eisenbach, L. & Lonai, P. (1992) *Development (Cambridge, U.K.)* **115**, 289–203.
6. Morrison-Graham, K., Schatteman, G. C., Bork, T., Bowen-Pope, D. F. & Weston, J. A. (1992) *Development (Cambridge, U.K.)* **115**, 133–142.
7. Schatteman, G. C., Morrison-Graham, K., Van Koppen, A., Weston, J. A. & Bowen-Pope, D. F. (1992) *Development (Cambridge, U.K.)* **115**, 121–131.
8. Chabot, B., Stephenson, D. A., Chapman, V. M., Besmer, P. & Bernstein, A. (1988) *Nature (London)* **335**, 88–89.
9. Geissler, E. N., Ryan, M. A. & Housman, D. E. (1988) *Cell* **55**, 185–192.
10. Tan, J. C., Nocka, K., Ray, P., Traktman, P. & Besmer, P. (1990) *Science* **247**, 209–212.
11. Stephenson, D. A., Mercola, M., Anderson, E., Wang, C., Stiles, C. D., Bowen-Pope, D. F. & Chapman, V. M. (1991) *Proc. Natl. Acad. Sci. USA* **88**, 6–10.
12. Smith, E. A., Seldin, M. F., Martinez, L., Watson, M. L., Choudhury, G. G., Lalley, P. A., Pierce, J., Aaronson, S., Barker, J., Naylor, S. L. & Sakaguchi, A. Y. (1991) *Proc. Natl. Acad. Sci. USA* **88**, 4811–4615.
13. Matthews, W., Jordan, C. T., Gavin, M., Jenkins, N. A., Copeland, N. G. & Lemischka, I. R. (1991) *Proc. Natl. Acad. Sci. USA* **88**, 9026–9030.
14. Geissler, E. N., McFarland, E. C. & Russell, E. S. (1981) *Genetics* **97**, 337–361.
15. Lyon, M. F. & Searle, A. G. (1989) *Genetic Variants and Strains of the Laboratory Mouse* (Oxford Univ. Press, Oxford), 2nd Ed.
16. Nocka, K., Majumder, S., Chabot, B., Ray, P., Cervonne, M., Bernstein, A. & Besmer, P. (1989) *Genes Dev.* **3**, 816–826.
17. Nocka, K., Tan, J. C., Chiu, E., Chu, T. Y., Ray, P., Traktman, P. & Besmer, P. (1990) *EMBO J.* **9**, 1805–1813.
18. Reith, A. D., Rottapel, R., Giddens, E., Brady, C., Forrester, L. & Bernstein, A. (1990) *Genes Dev.* **41**, 390–400.
19. Lyon, M. F. & Glenister, P. H. (1982) *Genet. Res.* **39**, 315–322.
20. Stevens, J. & Loutit, J. F. (1982) *Proc. R. Soc. London B* **215**, 405–409.
21. Duttlinger, R., Manova, K., Chu, T. Y., Gyssler, C., Zelenetz, A. D., Bachvarova, R. F. & Besmer, P. (1993) *Development (Cambridge, U.K.)* **118**, 705–717.
22. Tono, T., Tsujimura, T., Koshimizu, U., Kasugai, T., Adachi, S., Isozaki, K., Nishikawa, S., Morimoto, M., Nishimune, Y., Nomura, S. & Kitamura, Y. (1982) *Blood* **80**, 1448–1453.
23. Besmer, P., Manova, K., Duttlinger, R., Huang, E., Packer, A. I., Gyssler, C. & Bachvarova, R. (1993) *Development (Cambridge, U.K.)* **1993**, Suppl., 125–137.
24. Zelenetz, A. D., Chu, G., Galili, N., Bangs, C. D., Horning, S. J., Donlon, T. A., Cleary, M. L. & Levy, R. (1991) *Blood* **78**, 1552–1560.
25. Chu, T. Y. (1992) Ph.D. thesis (Cornell Univ. Graduate School of Medical Sciences, Ithaca).
26. Manova, K., Bachvarova, R. F., Huang, E., Sanchez, S., Velasquez, E., McGuire, B. & Besmer, P. (1992) *J. Neurosci.* **12**, 4363–4376.
27. Manova, K., Huang, E. J., Angeles, M., DeLeon, V., Sanchez, S., Pronovost, S. M., Besmer, P. & Bachvarova, R. F. (1993) *Dev. Biol.* **157**, 85–99.
28. Nagle, D. L., Martin-DeLeon, P., Hough, R. B. & Bucan, M. (1994) *Proc. Natl. Acad. Sci. USA* **91**, 7237–7241.